A Compact, High-Isolation Ultra-wideband two-port MIMO Antenna

Rahul Kumar Garg
Department of Computer Science and Engineering
University of Engineering & Management
Jaipur, India
rahulkumargarg08@gmail.com

Rahul Porwal
Department of Electronics and Communication Engineering
The LNM Institute of Information Technology
Jaipur, India
rahulporwal.y20@lnmiit.ac.in

Shipra Bhatia
Academy of Scientific and Innovative Research (AcSIR)
CSIR CEERI Pilani
Pilani, India
shiprabhatia94@gmail.com

M.V. Deepak Nair
Department of Electronics and Communication Engineering
The LNM Institute of Information Technology
Jaipur, India
deepak.nair@lnmiit.ac.in

***Abstract*— The present work suggests a miniature dual-element MIMO antenna for ultra-wide band (UWB) applications with high data-rates. The proposed antenna is designed to operate at 3.23-10.75 GHz with a 107.58% fractional bandwidth. The proposed MIMO setup consists of two same prototypes placed orthogonally in relation to one another and kept at a reasonable optimum distance. The isolation between the orthogonal antenna elements in the MIMO arrangement is more than 26 dB over the band. The antenna has a maximum gain of 5 dB with a stable radiation pattern and high isolation. The MIMO arrangement has an Envelope Correlation Coefficient (ECC) of less than 0.005 and a Diversity Gain (DG) of greater than 9.95. The fabrication and testing of the prototype validate the simulation results. The results indicate that the designed antenna can be beneficial for ultra-wideband and MIMO applications.**

Keywords*— Antenna, CPW feeding, Isolation, MIMO, ultra-wideband

I. INTRODUCTION

Ultra-wideband (UWB) technology with its wide frequency range of 3.1-10.6 GHz is appropriate for high-speed short-range wireless communications, radar, and medical imaging applications [1-2]. Microstrip patch antenna is a suitable option for UWB applications as it has a planar design, simple manufacturing process, and good integration capability with other electronic circuits [3]. Its compactness and usability with printed circuit boards (PCBs) make it even more desirable in portable and wearable technology. UWB design is challenging and is based on the accomplishment of wide impedance bandwidth, omnidirectional radiation patterns, miniaturized antenna design, and low signal distortion [4]. UWB Multiple-Input Multiple-Output (MIMO) antennas have drawn significant interest over the past few years due to their potential to enhance wireless communication systems through high data rates, high-quality signals, and consistent spatial diversity [5].

The design of UWB MIMO antennas focuses on compact size, broad impedance bandwidth, high isolation between the antenna elements, and uniform radiation patterns. Different techniques maximize these properties, such as decoupling structures, diversity schemes, and creative use of materials [6]. The integration of UWB and MIMO is famous for high data transmission rates, low power usage, and precise ranging. It enhances data rate and link quality through spatial diversity, leading to a powerful synergy for future wireless applications.

In the published literature, the researchers have been engaged in the development of different kinds of antennas for the UWB and MIMO applications. The design employs several novel geometries such as fractal, dipole, and Vivaldi. These are fed by numerous kinds of antenna feeding techniques, including symmetrical or asymmetrical CPW waveguide feed lines, microstrip feed lines, and using ground plane defects. In MIMO configuration, the literature suggests that the antenna placement, the use of various decoupling networks, resonant structure, metamaterial structure, EBG structure, etc., helps in achieving better isolation and reduced coupling between the antenna elements [7-20].

In this article, the authors have presented a compact UWB antenna and its MIMO configuration. The proposed antenna design achieves a broadband response using a simple microstrip line feed and a coplanar ground plane. With a bandwidth of 7.5 GHz, ranging from 3.2 GHz to 10.7 GHz, the antenna offers a maximum gain of 5 dBi. The two-port configuration of the antenna shows good MIMO characteristics. The observed values of the isolation, ECC, DG, and CCL are 26 dB, 0.005, 9.95, and 0.035 bits/sec/Hz, respectively. The radiation pattern of the design is nearly omnidirectional and remains stable across the operating bandwidth. The validity of the design results is confirmed through antenna prototyping and measurement.

II. ANTENNA DESIGN AND SIMULATION

A. Single Element Design

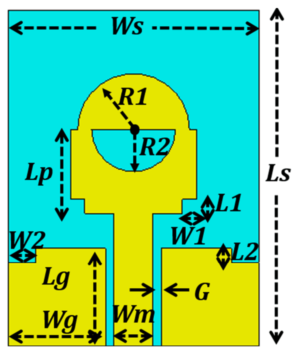

Fig. 1. Geometrical configuration of proposed UWB antenna. (where Ws=18, Wg=7, Wm=2.8, $W1$=1, $W2$=2, Ls=24, Lg=7, Lp=9, $L1$=1=$L2$, $R1$=4, $R2$= 3, and G= 0.6 (all are in mm)).

Fig. 1 depicts a schematic design of the proposed antenna with optimum design dimensions. The antenna is constructed with a FR-4 substrate with a loss tangent of 0.025, a thickness of 1.6 mm, and a relative permittivity of 4.4. It has a coplanar ground plane and is fed by a microstrip line. The antenna has dimensions of 18 × 24 mm^2. The radiating patch's shape has been modified, adjusted, and tuned to improve the antenna's performance within the FCC-approved UWB frequency range of 3.1 GHz to 10.6 GHz.

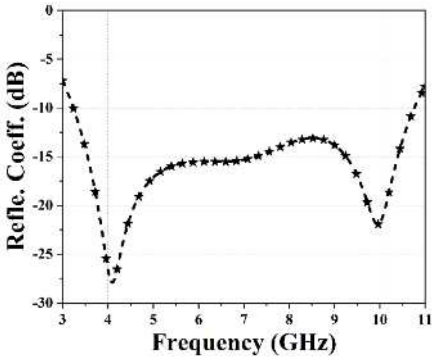

(a)

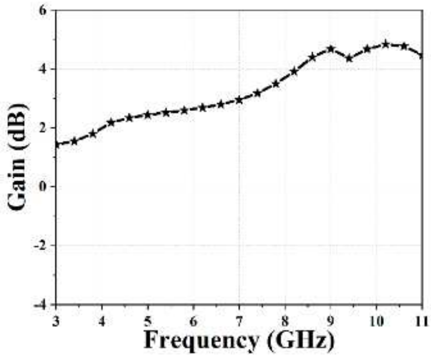

(b)

Fig. 2. Reflection Coefficient and gain performance of the antenna.

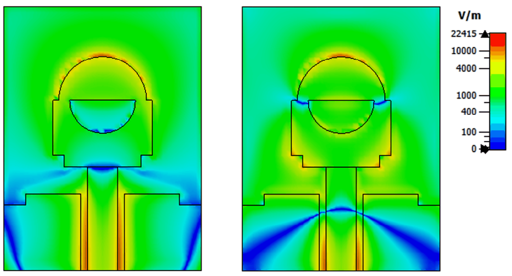

(a) 4.1 GHz (b) 9.9 GHz

Fig. 3. Surface current distribution of antenna.

A square patch is used as a starting point for the proposed structure, which has been tailored to provide a wider bandwidth response. This antenna has a 7.5 GHz bandwidth (3.2 GHz to 10.7 GHz) and a simulated gain of up to 5 dB. The antenna's gain increases in relation to the frequency. Fig. 2 showcases the proposed UWB antenna's reflection coefficient and gain curves. The distribution of surface currents at two different frequencies, 4.1 GHz and 9.9 GHz, is shown in Fig. 3. This picture provides essential insights into the antenna's design, leading to a better understanding of its physical properties. It is worth noting that current travels within the patch, feed line, and ground plane. The frequency that is chosen, though, affects the current distribution that each component experiences.

The proposed antenna's radiation patterns (2D and 3D) for strong resonances of the operational band are presented in Fig. 4. At the examined frequencies (4.1 GHz and 9.9 GHz), the patterns are nearly omnidirectional and stable throughout the operating bandwidth.

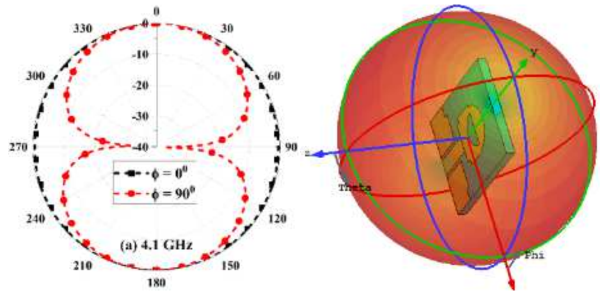

(a)

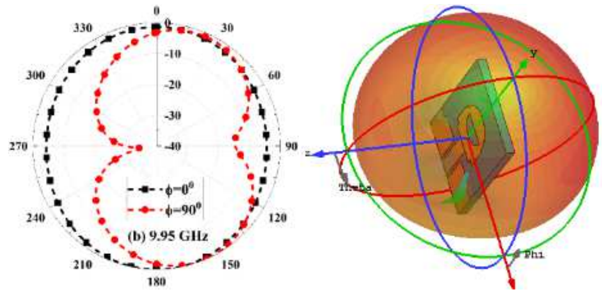

(b)

Fig. 4. The radiation patterns of the antenna at 4.1 GHz and 9.95 GHz.

B. MIMO Configuration

Fig. 5 depicts the designed antenna's MIMO configuration, comprising two replicated antenna elements laid out orthogonally to resemble polarization diversity. The MIMO antenna's dimensions are 24×52 mm^2. The antenna elements are separated by an optimum distance of $\lambda/2$.

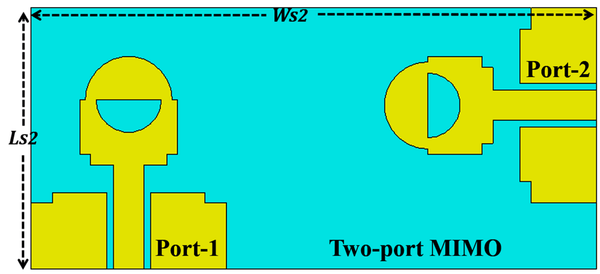

Fig. 5. MIMO configuration of the proposed antenna.

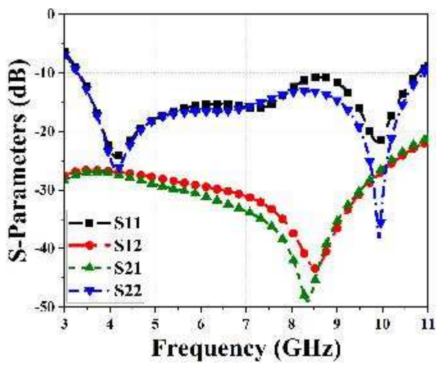

Fig. 6. S-parameters of the proposed MIMO antenna.

To evaluate design performance, the antenna's MIMO configuration is simulated. Due to the symmetry of both antenna elements, it is found that the reflection coefficient for both ports is identical. The impedance bandwidth of the MIMO antenna looks identical to that of a single antenna element. As seen in Fig. 6, the design offers at least 26 dB isolation. The improved isolation is due to the elements' orthogonal orientation and polarization diversity, lowering their coupling. Fig. 7 depicts the surface current distribution of the outlined MIMO antenna at a pair of distinct frequencies (4.1 GHz and 9.95 GHz), with one port being excited at once while the other port is connected with a 50-ohm load. When each port is exited individually, the surface current distribution for the specified frequencies travels across the patch, feed line, and ground planes.

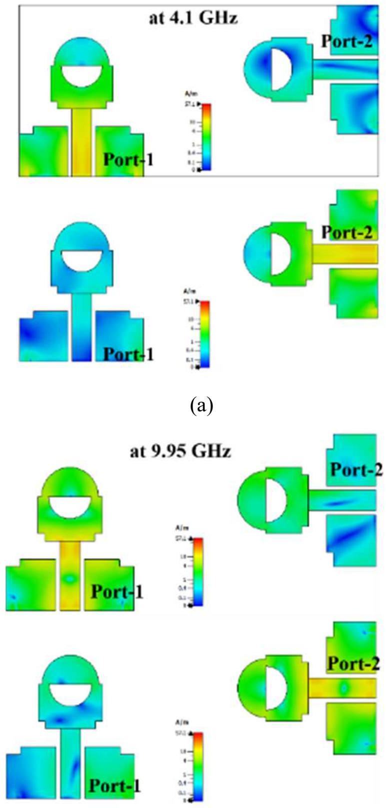

(a)

(b)

Fig. 7. Surface current plot of the proposed MIMO antenna.

Envelope Correlation Coefficient (ECC) and Diversity Gain (DG) are two parameters examined to determine the MIMO antenna's performance. The formulae for calculating these parameters are as follows [5]:

$$ECC_{ij} = \frac{|S_{ii}{}^{*}S_{ij} + S_{ji}{}^{*}S_{jj}|^2}{|(1 - |S_{ii}|^2 - |S_{ji}|^2).(1 - |S_{jj}|^2 - |S_{ij}|^2)|} \quad (1)$$

$$DG_{ij} = 10\sqrt{1 - |ECC_{ij}|^2} \quad (2)$$

where i and j are antennas for correlation, S_{ii} and S_{jj} are reflection coefficients of the ports, and S_{ij} and S_{ji} are isolation between the ports associated with the antenna structure. The DG and ECC graphs for the designed antenna with polarization diversity are shown in Fig. 8. ECC specifies how the signals that the antenna received are coupled. A lower correlation implies lower ECC. In practice, the maximal limit for ECC is set to 0.4. DG is another crucial factor that impacts MIMO operations. The DG will be higher if the ECC value is lower. A larger DG value ensures that MIMO behaves well.

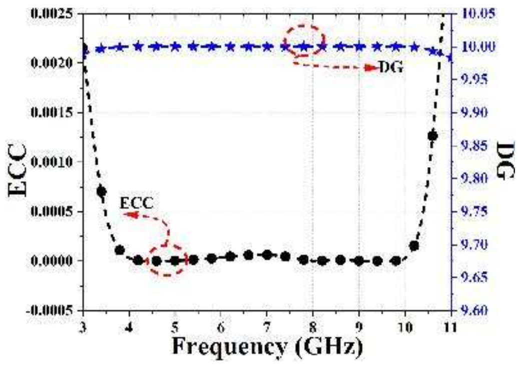

Fig. 8. MIMO Performance parameters.

III. PROTOTYPING AND MEASUREMENT

Prototypes of the said antenna and its MIMO setup are built, and the results are measured using the Vector Network Analyser VNA-ZNB40. The fabricated prototype and the setup for the measurement are shown in Fig. 9. The comparative study of the simulated and measured prototypes (single element and two-port MIMO design) is shown in Fig. 10. The measurement of the proposed designs are limited due to the limited facilities available. The outcomes of simulation and measurement appear to be in good alignment. The measured frequency band is between 3 GHz and 10.6 GHz. The measured isolation between antenna elements is greater than 26 dB over the working bandwidth, which is in accordance with the expected value. Minor variations between simulated and measured data may be identified as fabrication and soldering defects, and the available facilities impede the proposed design's measurement.

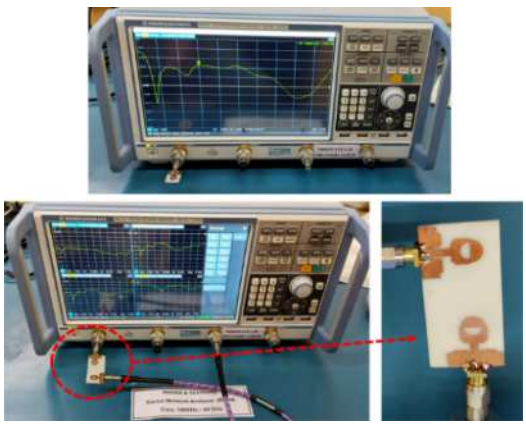

Fig. 9. Antenna prototype and measurement of results using VNA.

The antenna is compared to other designs that are currently accessible to review its performance and improvement. Table I illustrates the comparison. The proposed design has a wide operating bandwidth, comparatively lower dimensions, and comparable or better performance to the present study's findings. The fractional bandwidth (FBW) and bandwidth dimension ratio (BDR) are given as follows [11]:

$$FBW = 2 * \left\{\frac{f_H - f_L}{f_H + f_L}\right\} \quad (3)$$

$$BDR = \frac{FBW}{\lambda_0 \times \lambda_0} \quad (4)$$

TABLE I. COMPARISON OF LITERATURE AND THE PROPOSED WORK.

Ref.	Size		No. of Ports	B.W. (GHz)	FBW (%)	BDR	Isolation (dB)
	mm × mm	($\lambda_0\times\lambda_0$)					
[11]	19×30	0.196×0.31	2	3.1-10.6	109.4	1801	18
[12]	21.5×34	0.33×0.52	2	4.6-13.6	98.9	576.3	20
[13]	36×53	0.35×0.51	2	2.92-16.97	141.2	791.46	19
[14]	31×55	0.315×0.56	2	3.05-13.38	125.7	712.84	17
Here	24×52	0.258×0.56	2	3.23-10.75	107.58	744.61	26

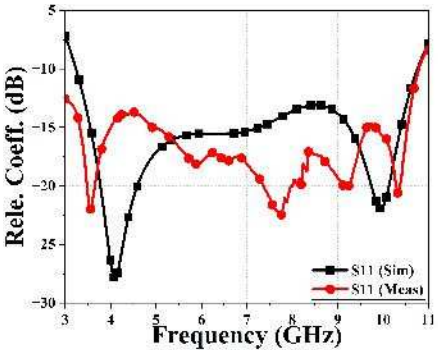

(a)

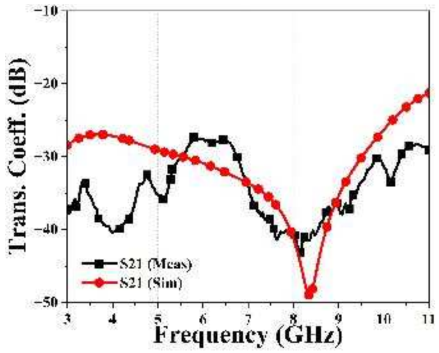

(b)

Fig. 10. Comparative study of the simulated and measured results.

IV. CONCLUSION

The current study employs a compact antenna and its two-port MIMO configuration for ultra-wideband applications. The proposed design has a bandwidth of 3.23 GHz to 10.75 GHz in simulation and is validated in the measurement. The MIMO design has an overall footprint of 24×52 mm^2 (0.258 mm × 0.56 mm at the largest wavelength). The design has a fractional bandwidth of 107.58% and a BDR of 744. The two-port MIMO configuration shows that the isolation between the antenna elements is more than 26 dB throughout the operating bandwidth, similar to the single-element design. The other MIMO parameters were observed to be well within the range suggested in the literature (ECC and DG were 0.005 and 9.95, respectively). The prototypes with optimal specs for the designs have been fabricated and tested. The measured data shows an acceptable alignment with the simulated result. The proposed design is suitable for the ultra-wideband and MIMO applications.

ACKNOWLEDGEMENT

The authors acknowledge the ECE Department at the LNM Institute of Information Technology in Jaipur, India, for assistance and direction with prototype fabrication facilities and testing.

REFERENCES

[1] G. Breed, “A summary of FCC rules for ultra wideband communications,” *High Frequency Electronics*, vol. 4, no. 1, pp. 42–44, 2005.

[2] F. Standard, “First-order and report, revision of part 15 of the commission’s rules regarding UWB transmission systems,” 2002.

[3] W. Balani, M. Sarvagya, T. Ali, M. P. MM, J. Anguera, A. Andujar, and S. Das, “Design techniques of super-wideband antenna–existing and future prospective,” *IEEE Access*, vol. 7, pp. 141241–141257, 2019.

[4] H. G. Schantz, “A brief history of UWB antennas,” *IEEE Aerospace and Electronic Systems Magazine*, vol. 19, no. 4, pp. 22–26, 2004.

[5] M.S. Sharawi, “Printed MIMO antenna engineering”, *Artech House*, 2014.

[6] R. Cicchetti, E. Miozzi, O. Testa, “Wideband and UWB antennas for wireless applications: A comprehensive review”, *International Journal of Antennas and Propagation*, no. 1 (2017): 2390808.

[7] P. Kumar, M.M.M. Pai, T. Ali, “Ultrawideband antenna in wireless communication: A review and current state of the art”, *Telecommunications and Radio Engineering*, vol. 79, no. 11, pp. 929-942, 2020.

[8] P. Sharma, R.N. Tiwari, P. Singh, P. Kumar, B.K. Kanaujia, “MIMO antennas: Design approaches, techniques and applications”, *Sensors* 22, no. 20 (2022): 7813.

[9] I. Gnanaharan, R. Anbazhagan, “Review on the Design of the Isolation Techniques for UWB-MIMO Antennas”, *Advanced Electromagnetics*, vol. 7, no. 4, pp. 46-70, 2018.

[10] R. Kumar, *et al.*, “Mutual coupling reduction techniques for UWB-MIMO antenna for band notch characteristics: A comprehensive review”, *Wireless Personal Communications*, Vol. 131, no. 2, pp. 1207-1247, 2023.

[11] A. Kumar, A.Q. Ansari, B.K. Kanaujia, J. Kishor, S. Kumar, “An ultra-compact two-port UWB-MIMO antenna with dual band-notched characteristics”, *AEU-international Journal of Electronics and Communications*, Vol. 114, 152997, 2020.

[12] V.K. JhunJhunwala, P. Kumar, Bharathi R.B., K.M. Nayak, S. Pathan, Subhash B.K., O.P. Kumar, T. Ali, “A Novel Elliptical-Shaped UWB Two-Port MIMO Antenna With Enhanced Isolation for Wireless Application”, *Journal of Electrical and Computer Engineering,* no. 1 (2025): 6617657.

[13] S. Yao, X. Qiu, T. Yang, “A Miniaturized UWB MIMO Antenna Design for 5G Multi-Band Applications”, *Progress In Electromagnetics Research C*, Vol. 153, pp. 1-12, 2025.

[14] S. Yao, T. Yang, X. Qiu, X. Li, “A Frog-Shaped UWB MIMO Antenna Design for 5G”, *Progress In Electromagnetics Research C*, Vol. 151, pp. 101-112, 2025.

[15] G.S. Patnaik, D.C. Panda, D.K. Naik, “UWB MIMO Antenna Using h-Shaped Fractals”, *IEEE 4th International Conference on Applied Electromagnetics, Signal Processing, & Communication* (*AESPC*), 2024.

[16] N. Dalakoti, P. Jain, “Frequenz: A compact dual-element UWB-MIMO antenna with single band-notched characteristics”, 2024.

[17] P. Chaudhary, A. Kumar, R.K. Arya, M. Ali, “Metamaterial-inspired UWB MIMO antenna with polarization diversity”, *AEU - International Journal of Electronics and Communications*, Vol. 187, December 2024, 155518.

[18] K.V. Prasad, T. Haritha, V.S.D. Rekha, B. Alekhya, V. Saritha, “Isolation Improvement of UWB-MIMO Design Using Elliptical Stub”, *IETE Journal of Research*, Vol. 71, Issue 1, 2025.

[19] D. Singh, M. Särestöniemi, T. Myllyla, “Analysis of Various Methods to Boost the Isolation in UWB-MIMO Antennas”, *In Intelligent*

Circuits and Systems for SDG 3–Good Health and well-being, pp. 110-118. CRC Press, 2024.

[20] A.H. Elnaggar, A.S. Abd El-Hameed, M.A. Yakout, N.F.F. Areed, "Development and comprehensive evaluation of a dual-port textile UWB MIMO antenna for biomedical use", *Optical and Quantum Electronics*, Vol. 56, article number 1099, 2024.